AQUA
Water Infrastructure, Ecosystems and Society

 AQUA — Water Infrastructure, Ecosystems and Society Vol 71 No 4, 533 doi: 10.2166/aqua.2022.157

# Assessment of M5 model tree for prediction of azithromycin antibiotic removal by multi-wall carbon nanotubes in a fixed-bed column system

Mohammad Javad Amiri *, Mehdi Bahrami and Sara Rajabi
Department of Water Engineering, College of Agriculture, Fasa University, Fasa 74616-86131, Iran
*Corresponding author. E-mail: mj_amiri@fasau.ac.ir

MJA, 0000-0002-2633-0572

## ABSTRACT

In this research, an M5 model tree is employed for the prediction of removal efficiency of azithromycin antibiotics by multi-wall carbon nanotubes (MWCNTs), based on experimental data sets from a laboratory column mode. The effect of total flow time (0–260 min), influent flow rates (0.5, 1, and 1.5 mL $min^{-1}$), bed depths (2, 4, and 6 cm), initial azithromycin concentrations (25, 50, and 100 mg $L^{-1}$), and pHs (2, 4, 6, 8, and 10) was considered in the adsorption process. Based on the obtained structures, three linear equations (LM, LM2, and LM3) were developed. The root mean square error (RMSE) of 9.89% and determination coefficient ($R^2$) of 0.946 were determined for predicting azithromycin removal by the M5 model tree. The results indicated that contact time was more important in the adsorption process, relative to other operating conditions. This research showed that the M5 model tree could be an accurate and faster alternative to the available mathematical models to estimate removal rates of pollutants. The results obtained from the FTIR technique confirmed that the O–H groups on the MWCNTs surface have an important role in azithromycin adsorption.

**Key words:** adsorption process, mathematical model, operating condition, removal efficiency

## HIGHLIGHTS

- Fixed-bed column modeling was performed by the M5 model tree.
- Azithromycin removal by MWCNTs is more sensitive to contact time.
- Model predictions were in agreement with experimental data at diverse operational conditions.
- The results obtained from the Yoon–Nelson model confirmed the results from the M5 model.
- O–H groups have an important role in azithromycin adsorption.

## GRAPHICAL ABSTRACT

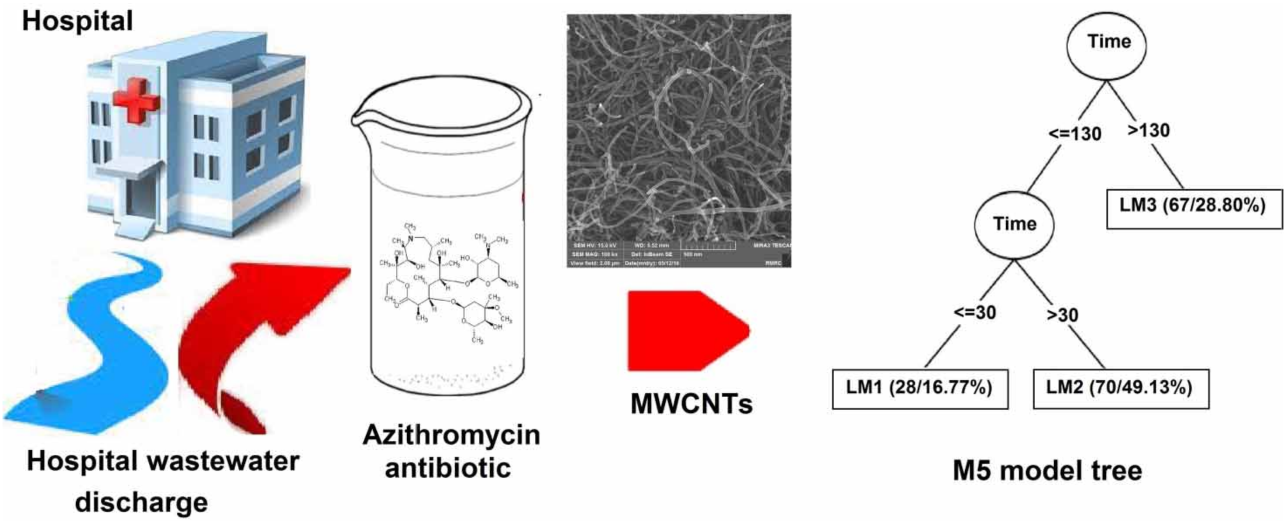


## INTRODUCTION

In recent years, the high global utilization rate of pharmaceuticals by humans and animals has led to the contamination of the environment (Fonseca *et al.* 2020). Pereira *et al.* (2020) reported that antibiotics, anti-inflammatories, antiepileptics, and hormones are four common pharmaceuticals that caused the highest ecological risks. Antibiotics are organic compounds that have been widely applied for treatment and/or inhibition of bacterial infections in humans and animals as well as for agricultural purposes (Al-Riyami *et al.* 2018). The steady discharge of antibiotics from the pharmaceutical industries, households, and hospitals into the environment can cause an emerging contaminant in aquatic environments and pose potential hazards to humans (Sadeghi *et al.* 2018).

Azithromycin is a macrolide-type antibiotic designed to overcome some of the drawbacks of erythromycin, including drug sensitivity and its limited antimicrobial spectrum. Azithromycin is also prescribed to treat bacterial infections such as bronchitis, skin infections, respiratory infections, and sexually transmitted infections (Alvarez-Elcoro & Enzler 1999).

Azithromycin is a non-biodegradable antibiotic that cannot be effectively removed by conventional wastewater treatment in the purification process (Kamani *et al.* 2017). Hence, finding a suitable method for the complete elimination of this substance from the natural environment should be considered. Although the concentration of this substance in water is in the range of micrograms to nanograms, its storage in animals and human bodies leads to various diseases. In recent years, advanced technologies such as chemical oxidation using ozone and ozone/hydrogen peroxide (Cuerda-Correa *et al.* 2020; Rekhate & Srivastava 2020), membrane filtration such as nanofiltration and reverse osmosis (Nghiem *et al.* 2005), and adsorption with carbon materials (Babaei *et al.* 2016; Takdastan *et al.* 2016) and nanomagnetic materials (Mohammadi *et al.* 2020) were employed to eliminate the antibiotic pollutants from aqueous media. Liu *et al.* (2019) found out that the combination of UV with ozone/$H_2O_2$ is an efficient advanced oxidation process (AOP) for the degradation of micropollutants. Based on Salvestrini *et al.* (2020), the commercial activated carbon was successfully used to adsorb micropollutant up to 180 mg $g^{-1}$ in terms of the Diffusion-Controlled Langmuir Kinetic (DCLK) model. Gallo-Cordova *et al.* (2021) claimed that the iron oxide magnetic nanocatalyst in AOP improved the degradation of real wastewaters containing organic pollutants.

Among the various treatment methods, the adsorption process with low cost, high efficiency, and versatile adsorbents is an effective elimination procedure in reducing the target pollutants such as antibiotics (Babaei *et al.* 2016; Takdastan *et al.* 2016; Gholamian *et al.* 2021), diclofenac (Salvestrini *et al.* 2020), herbicide (Amiri *et al.* 2020), caffeine (Bahrami *et al.* 2017), benzene/toluene in single and binary systems (Erto *et al.* 2017), and heavy metals (Bassyouni *et al.* 2020). One of the most widely used adsorbents in the removal of pharmaceutical compounds from aquatic environments is nanostructured materials like carbon nanotubes (CNTs) (Zhang *et al.* 2011; Babaei *et al.* 2016). The application of CNTs to eliminate pharmaceutical compounds (Zhang *et al.* 2011; Kim *et al.* 2014), pesticides (Uddin 2021), herbicides (Amiri *et al.* 2018a; Bahrami *et al.* 2018), dyes (Dutta *et al.* 2018), and heavy metals (Bassyouni *et al.* 2020) has been satisfactorily employed. Due to the unique physical and chemical characteristics of CNTs consisting of a high specific surface area, tunable surface chemistry, a layered and hollow structure, and high regeneration capacity, this adsorbent is attractive to use extensively for environmental remediation (Zhang *et al.* 2011; Qu *et al.* 2013). One of the most widely used types of CNTs is multi-walled carbon nanotubes (MWCNTs) that are successfully applied in the elimination of various contaminations such as pharmaceuticals products (Wang *et al.* 2016), caffeine (Bahrami *et al.* 2017), and herbicides (Amiri *et al.* 2018a; Bahrami *et al.* 2018) from aqueous solutions.

Continuous adsorption in a packed column is worthwhile from the industrial point of view because this system increases the contact between pollutant and adsorbent and can be scaled up to industrial size from the laboratory process (Amiri *et al.* 2017a). The main effective factors on adsorption process in a packed column are temperature ($T$), reaction time ($t$), acidity (pH), bed height ($h$), inflow rate ($q$), and the initial concentration of the contaminant ($c$), which have complicated relationships with adsorption capacity (Amiri *et al.* 2017b). So, theoretical (Amiri *et al.* 2018b; Amiri & Noshadi 2020) and artificial intelligence (Amiri *et al.* 2017b, 2019) models are used to simulate and estimate the impact of each input factor on the adsorption. However, these models have limitations for predicting the breakthrough curves under various operating conditions.

The M5 model tree as a usual decision tree with a linear regression function at the terminal nodes is a subset of machine learning and data mining techniques, which is used to make a relationship between independent and dependent factors (Goyal 2014). The M5 tree network model has been satisfactorily employed in modeling and approximating complex non-linear systems in various fields of water engineering such as flood predicting water level-discharge relationship, rainfall-runoff simulation, sedimentation modeling, and $ET_o$ approximation (Rahimikhoob 2014).

Therefore, the main aim of this research was to investigate the possibility of using MWCNT as adsorbent to remove azithromycin from aqueous media in a continuous adsorption system. The specific aim of this research was to study the accuracy of an M5 approach for adsorption modeling and to compare this with the performance of the commonly used Yoon–Nelson empirical model.

## MATERIALS AND METHODS

### Chemicals

Azithromycin powder (≥97%) was provided from Tehran Chemie Pharmaceutical Company. MWCNTs with physical characteristics of diameter 10–20 nm, length 30 μm, specific surface area 200 $m^2\,g^{-1}$, and density 2.1 g $cm^{-3}$ were purchased from the Belgian company, Nanosil. Other chemicals (HCL, 37%; NaOH, ≥99%) were provided from Sigma-Aldrich Co. All chemical reagents were of analytical grade. The details for analytical techniques are provided in the Supplementary material.

### Column experiments

A fixed-bed column system was designed to investigate the removal of azithromycin by MWCNTs. Continuous flow measurements were carried out in a glass column with a height of 25 cm and an inner diameter of 2 cm. Two layers of glass beads were placed at the beginning and end of the column to support the adsorbent as seen in Supplementary Material, Figure S1. Azithromycin solution with different initial concentrations (25, 50, and 100 mg $L^{-1}$) was passed through the column with various bed depths (2, 4, and 6 cm) using a peristaltic pump at several influent flow rates (0.5, 1, and 1.5 mL $min^{-1}$) and pHs (2, 4, 6, 8, and 10). Liquid samples were taken from the exit of the column at certain time intervals and analyzed for azithromycin concentration. The column tests were stopped when the MWCNTs were completely saturated. Each column test was performed in triplicate and the average of the results was recorded.

### Column data analysis

The azithromycin removal ($R$, %) can be obtained from the ratio of the total quantity of azithromycin adsorbed in the column ($m_{ad}$, mg) to the total quantity of azithromycin sent through the column ($m_{ad}$, mg) as follows:

$$R = \frac{m_{ad}}{m_{total}} \times 100 = \frac{q \times \int_{t=0}^{t=t_e} C_{ad} dt}{\frac{C_o \times q \times t_e}{1000}} \times 100 \tag{1}$$

where $C_{ad}$ and $C_o$ are the adsorbed and initial azithromycin concentration (mg $L^{-1}$), $q$ is the flow rate, and $t_e$ is the column exhaustion time (min) (the time at which azithromycin concentration in the outlet reached 99.5% of inlet azithromycin concentration).

### Isotherms and kinetic studies

Two well-known isotherm models (Langmuir and Freundlich) were used to fit the equilibrium data for a better understanding of the adsorption process by mixing 0.1 g of MWCNTs with 100 mL of various azithromycin concentrations ranging from 5 to 100 mg $L^{-1}$. Moreover, two common kinetic models (Pseudo-first-order and Pseudo-second-order) were also employed to fit the experimental data at different values of contact time (0, 20, 40, 60, 80, 100, 120, 140, 160, 180, 200, 220, 240, and 260 min). All the investigated mathematical models are summarized in Supplementary Material, Table S1 and more details are provided by Babaei *et al.* (2016).

### M5 model tree

The applicability of the M5 model was studied to estimate the removal efficiency of azithromycin by MWCNTs in a fixed-bed column system. The M5 model tree as one of the data mining techniques is a common decision tree with a linear regression function at the terminal nodes, which was first introduced by Quinlan (1992). This model, unlike the other decision-making trees that are used for predicting discrete classes, can be used for predicting continuous numerical variables. Model tree generation involves two stages: the first step includes setting a division criterion for establishing the decision-making tree, whereas the second step involved a pruning method for pruning the overgrown trees. The M5 model tree algorithm uses the standard deviation of the values in the subset of examples as a splitting criterion to identify the node that expresses the desired standard error. The model calculates the minimum expected error as a test result in that node. The standard deviation reduction (SDR) used in the design of the M5 model tree can be expressed by the following equations (Rahimikhoob 2014):

$$\mathrm{SDR} = sd(T) - \left( \sum_{i=1}^{N} \frac{|T_i|}{|T|} sd(T_i) \right) \tag{2}$$

$$sd(T) = \sqrt{\frac{\sum_{i=1}^{N} y_i^2}{N} - \left( \frac{\sum_{i=1}^{N} y_i}{N} \right)^2} \tag{3}$$

where $T$ and $T_i$ represent a set of examples that reaches the node and the subset of examples that have the $i$th outcome of the potential set, respectively. $sd$ represents the standard deviation, $y_i$ represents the numerical value of the objective property of the sample $i$, and $N$ is the data number.

The splitting process is repeated many times in each node to reach the final node. M5 chooses the one split that maximizes the expected error reduction. This data division during the M5 model creation frequently produces a large tree structure which may over-fitting the training data and cause poor generalization performance in the testing stage. To resolve this drawback, Quinlan (1992) has suggested the use of a pruning method to prune back the overgrown tree. In general, this pruning method is obtained by substituting the sub-tree with linear regression functions. Figure 1 indicates splitting the input space $X1 \times X2$ as the independent variables into four leaves with a linear regression function at the leaves (LM1 through LM4) by the M5 model tree algorithm. WEKA software (Witten & Frank 2005) is employed to model the M5 method.

### Weka software

The Weka software as a tool for data processing was first implemented in 1992 to compile and integrate machine learning algorithms using JAVA (Witten & Frank 2005). This software was upgraded to a general data mining license in 1993. Currently, this software contains a large number of machine learning and data mining techniques that allow the users to compare different machine learning techniques. In this study, the operating parameters in a fixed-bed column system such as total flow time ($t$), influent flow rate ($q$), bed depth ($h$), initial azithromycin concentration ($c$), and pH were introduced as input data to Weka software and the azithromycin removal as the software output. Then, out of 165 experimental data, 70% of the data equal to 116 data were selected as training data and 30% of the data equal to 49 data were selected as test data. After implementation, the model was evaluated using evaluation criteria.

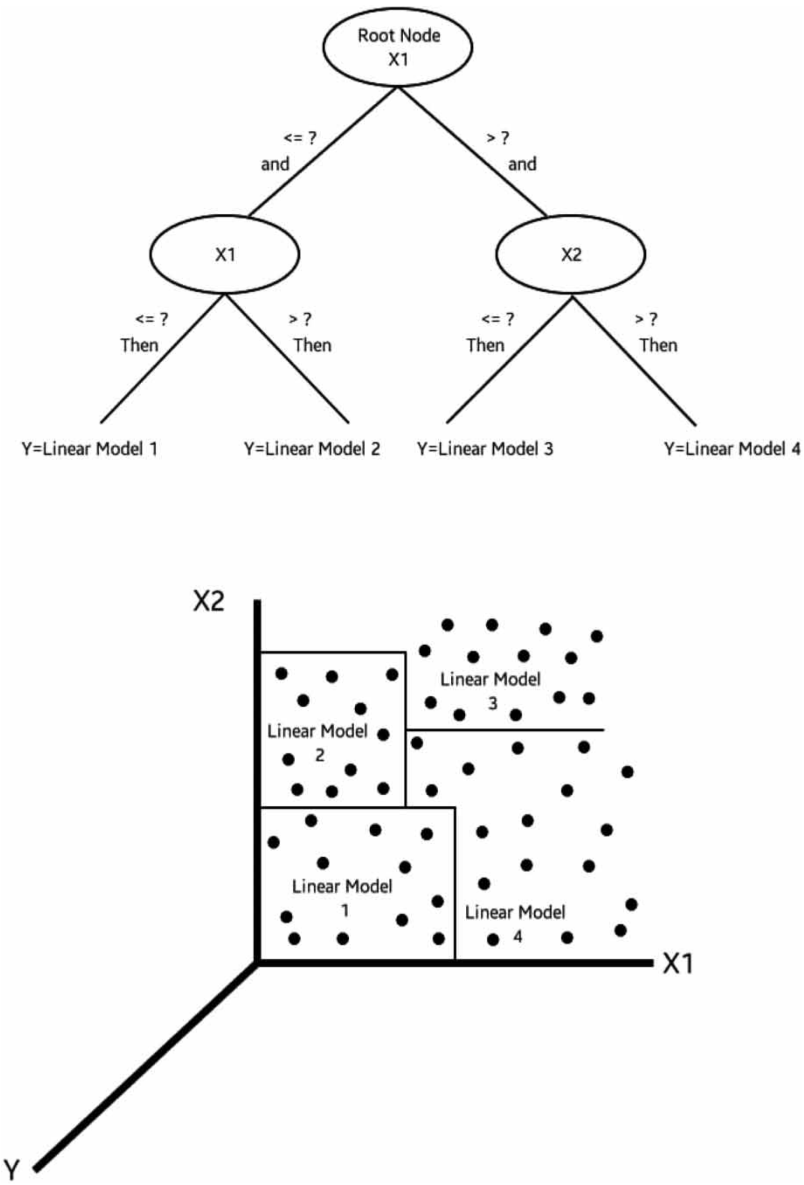


**Figure 1** | Splitting the input space by the M5 model tree algorithm.

## Evaluation criteria

To assess the performance of M5 model in azithromycin removal prediction, two evaluation criteria consisting of root mean square error (RMSE) and coefficient of determination ($R^2$) were applied as follows (Amiri *et al.* 2020):

$$\mathrm{RMSE} = \left[\frac{\sum_{i=1}^{n}[(R)_{\mathrm{pre}} - (R)_{\mathrm{mea}}]^2}{n}\right]^{0.5} \tag{4}$$

$$R^2 = \frac{\sum_{i=1}^{n}[[(R)_{\mathrm{pre}} - (\overline{R})_{\mathrm{pre}}][(R)_{\mathrm{mea}} - (\bar{R})_{\mathrm{mea}}]]}{\sum_{i=1}^{n}[(R)_{\mathrm{mea}} - (\overline{R})_{\mathrm{mea}}]^2 \sum_{i=1}^{n}[(R)_{\mathrm{pre}} - (\bar{R})_{\mathrm{pre}}]^2} \tag{5}$$

where $(R)_{mea}$ and $(R)_{pre}$ are measured and predicted removal efficiency of azithromycin in a fixed-bed column system, respectively, $(\overline{R})_{mea}$ and $(\overline{R})_{pre}$ are the mean of the measured and predicted azithromycin removal efficiency, respectively, and $n$ is the data number.

### Data analysis

The statistical analysis of data was done by SPSS 16 software and the comparison of means was performed using the Duncan test at a significance level of 5%.

## RESULTS AND DISCUSSION

### Characterization of MWCNTs

MWCNTs were provided with diameters in the range of 10–20 nm, lengths of 30 μm, and densities of 2.1 g $cm^{-3}$. The average pore diameter of MWCNTs was 7.2 nm, which showed that the diameter of the pores is between 2 and 50 nm suggesting mesoporous structures. The specific surface area and pore volume of MWCNTs were 200 $m^2$ $g^{-1}$ and 0.348 $cm^3$ $g^{-1}$, respectively, which indicate that the MWCNTs are a good candidate to remove antibiotic pollutants (Wang *et al.* 2016). MWCNTs are black powder (see Figure 2(a)) with $pH_{PZC}$ of 4.1. At pH < 4.1, the net charge of the MWCNTs is positive, whereas at pH > 4.1 the net charge of the MWCNTs is negative (see Figure 2(b)). The SEM images of the MWCNTs at different magnifications indicate that this material has a tubular shape with a well-developed porous structure (see Figure 2(c)). The FTIR spectrum of the MWCNTs indicates a broad peak at 3,440 $cm^{-1}$, which corresponds to hydroxyl groups. The band at about 2,800–3,000 $cm^{-1}$ is assigned to the $CH_x$ groups (Bahrami *et al.* 2017). The band at 1,740 $cm^{-1}$ was assigned to COOH groups and the peak at 1,638 $cm^{-1}$ is due to the C = C stretching mode (Amiri *et al.* 2018a). Moreover, the band at 1,275 $cm^{-1}$ is attributed to C–O stretching band (see Supplementary Material, Figure S2). The peak shapes in the FTIR spectra of MWCNTs were dramatically changed after azithromycin adsorption (see Figure 2(d)). After azithromycin adsorption, the peaks of the hydroxyl groups are stronger than before adsorption, which could be related to the formation of some

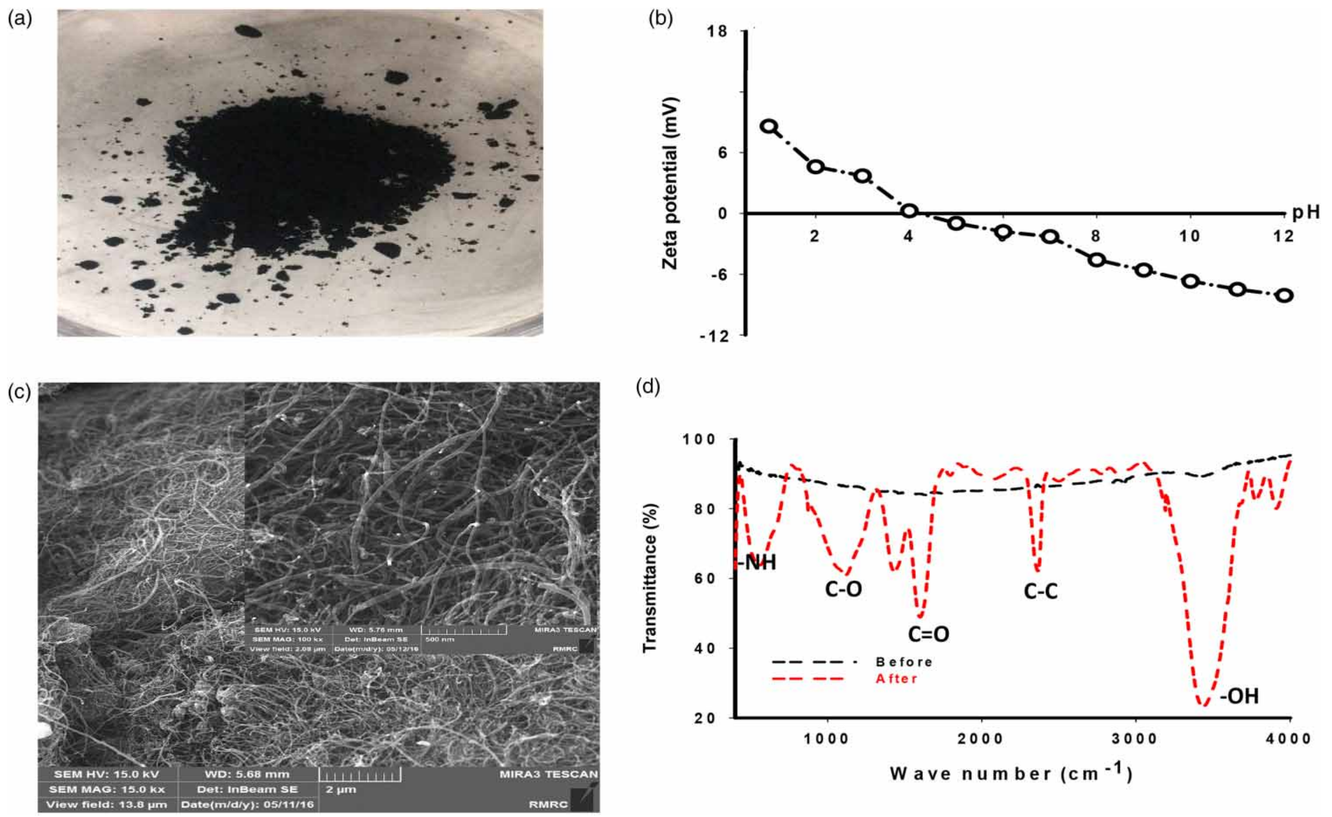


**Figure 2** | Characterization of MWCNTs: the photography of sample (a), the Zeta potential of sample (b), SEM image of the sample (c), and FTIR spectra of the sample before and after the azithromycin adsorption (d).

new oxygen-containing functional groups on the MWCNTs surfaces, which increase the hydrophilic properties of MWCNTs and act as binding sites to remove azithromycin.

## Effect of operating parameters

Eleven series of column experiments were carried out in triplicate at diverse operating conditions (see Supplementary Material, Table S2). The effect of various initial solution pH from 2 to 10 with a constant value of initial azithromycin concentration (50 mg $L^{-1}$), bed depth (4 cm), and flow rate (1 mL $min^{-1}$) is illustrated in Figure 3(a). As can be seen in Figure 3(a), in greater solution pH, the adsorption process achieved saturation faster and both breakthrough time (the time that $C_t/C_o = 0.05$) and exhaustion time increased. The increasing trend of azithromycin elimination by MWCNTs with rising the solution pH might be related to the fact that $pH_{PZC}$ (4.1) of MWCNTs is lower than the pKa (8.74) of azithromycin (Davoodi *et al.* 2019). At pH < 4.1, the MWCNTs surface protonates and becomes positively charged, whereas at pH > 4.1, the MWCNTs surface deprotonates and becomes negatively charged. Around pH 10, cationic species of azithromycin molecules were dominant and the surface of MWCNTs was negative. Hence, the electrostatic attraction might occur between them and result in higher adsorption capacity (Amiri *et al.* 2017a; Davoodi *et al.* 2019). In the study led by Gholamian *et al.* (2021), the optimum pH value for azithromycin removal by silica SBA-15 was achieved at 8.25. According to Supplementary Material, Table S3, there is a significant difference at pH 8 in the performance of the dynamic adsorption process with other pH treatments. Davoodi *et al.* (2019) concluded that 92 and 79% removal of azithromycin were achieved by saponin-modified nano diatomite at pH 11 and 9, respectively, within the 60-min contact time.

The effect of flow rate between 0.5 and 1.5 mL $min^{-1}$ was investigated, while the initial concentration of azithromycin (50 mg $L^{-1}$), bed height (4 cm), and pH (6) were kept constant (see Figure 3(b)). According to Supplementary Material, Table S3,

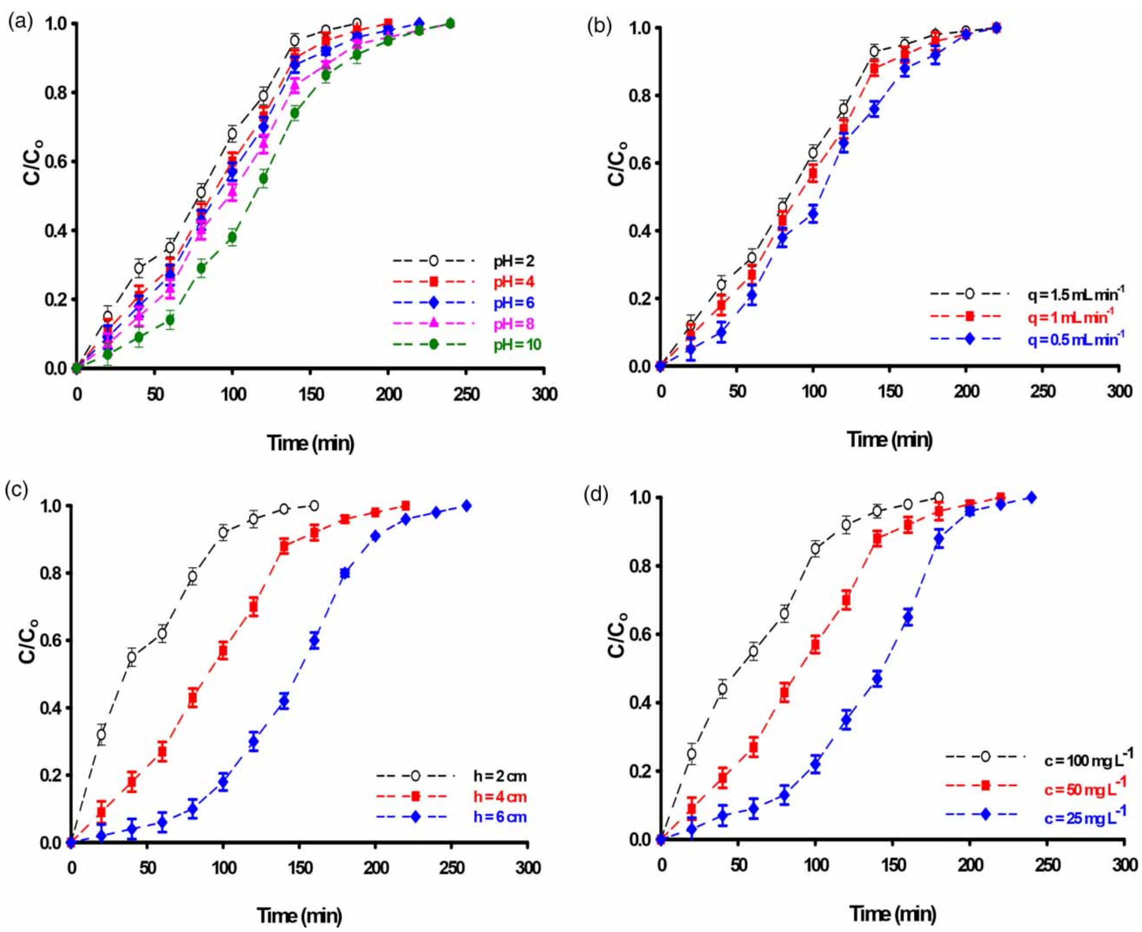


**Figure 3** | Breakthrough curves of azithromycin as a function of pH (a), flow rates (b), bed depths (c), and initial concentrations (d).

the effect of feed flow rate change on breakthrough curves is significant at the 5% level by Duncan tests. It can be seen that an increase in flow rate from 0.5 and 1.5 mL $min^{-1}$ reduced both breakthrough and exhaustion times and consequently decreased the adsorption efficiency of azithromycin. This can be attributed to the fact that at a greater flow rate, azithromycin molecules have less time to diffuse into the MWCNTs pores and the contact time of the azithromycin in the column was not long enough to reach adsorption equilibrium (Amiri *et al.* 2017a, 2020; Bahrami *et al.* 2018). Similar findings have been reported in the study by Hu *et al.* (2020) for the phosphate adsorption by granular acid-activated neutralized red mud at various flow rates (0.5, 1.0, and 2.5 mL $min^{-1}$).

The effect of different bed depths from 2 to 6 cm on the breakthrough curves is investigated, when the initial azithromycin concentration (50 mg $L^{-1}$), flow rate (1 mL $min^{-1}$), and pH (6) were fixed (see Figure 3(c)). According to Supplementary Material, Table S3, the variation of bed depths has a statistical influence for dynamic adsorption of azithromycin in a fixed-bed column system. From Figure 3(c), when the MWCNTs bed height increases, both breakthrough and exhaustion times shift to the right side and consequently the removal efficiency of azithromycin increases. In fact, with rising bed depth from 2 to 6 cm, the number of available active sites on the MWCNTs surfaces enhanced and consequently the reaction time between azithromycin molecules and the MWCNTs increased, which result in to increase removal efficiency (Amiri *et al.* 2020; Hu *et al.* 2020). Similar results were found in the study by Babaei *et al.* (2016), who showed that the adsorption percentage of tetracycline increased with an increase in the MWCNT dosage. Gholamian *et al.* (2021) reported the maximum azithromycin adsorption of 83.3% under the optimum silica SBA-15 dosage of 1.55 g $L^{-1}$.

The influence of different initial azithromycin concentrations on the breakthrough curves was studied at a bed depth of 4 cm, a flow rate of 1 mL $min^{-1}$, and a pH of 6 (see Figure 3(d)). Breakthrough curves were not significantly different in treatments 50 and 100 mg $L^{-1}$, but the difference between them was significant with treatment of 25 mg $L^{-1}$ (Supplementary Material, Table S3). As expected, with increasing azithromycin concentration from 25 to 100 mg $L^{-1}$, the volume of the azithromycin solution introduced into the column increased, and the breakthrough curve was transferred to the origin; consequently, the removal efficiency decreased. In fact, at high azithromycin concentration, the concentration gradient between MWCNTs and azithromycin solution was increased, which result in faster saturation of the MWCNTs active sites and reduced both breakthrough and exhaustion times (Bahrami *et al.* 2018; Amiri *et al.* 2020; Hu *et al.* 2020). Based on Wang *et al.* (2016), the removal ratios of triclosan, prometryn, 4-acetylamino-antipyrine, carbendazim, caffeine, ibuprofen, and acetaminophen were 0.93, 0.71, 0.67, 0.65, 0.42, 0.34, and 0.29 by MWCNT at a feed concentration of 1 mg $L^{-1}$. Davoodi *et al.* (2019) found the maximum uptake capacity of saponin-modified nano diatomite at 100 mg $L^{-1}$ initial azithromycin concentration was 79 mg $g^{-1}$ at a contact time of 60 min.

The variations of azithromycin removal efficiency with contact time in continuous adsorption system as a function of pH (see Figure 4(a)), flow rates (see Figure 4(b)), bed depths (see Figure 4(c)), and initial concentrations (see Figure 4(d)) are illustrated in Figure 4. As can be seen in Figure 4, the initial rate of adsorption was very rapid and gradually decreased with the saturation of MWCNTs active sites, and then equilibrium was achieved. Kim *et al.* (2014) claimed that the adsorption of two antibiotics including lincomycine and sulfamethoxazole onto carbon materials occurred with quick initial adsorption to the outer surface, followed by a slow diffusion.

## Modeling results

The results of applying the M5 tree model in predicting the removal efficiency of azithromycin have led to the creation of three linear equations as shown in Figure 5. In the proposed tree model, if the time is less than or equal to 30 min, more than 30 min, and more than 130 min, the removal efficiency of azithromycin will be calculated using the linear equations LM, LM2, and LM3, respectively. These linear equations are presented in certain intervals of the input data. The numbers in parentheses in linear equations of the M5 tree model image show the number of items of data that apply to each linear relation. It is obvious that some of the operating factors would play a more important role than others and it is essential that only the significant ones be applied as inputs to the M5 model. As can be seen, the removal efficiency of azithromycin is a function of time and among all the input parameters of the model, which included reaction time, influent flow rate, bed height, pH, and initial azithromycin concentration, the output is only in terms of time. The reaction time was only the significant factor, whereas the other parameters did not have a significant effect on the removal efficiency of azithromycin and consequently were not included in the final removal efficiency equation. The results indicated that the $R^2$ and RMSE values for the relationship between the M5 model-estimated and measured data at the testing stage were 0.946 and 9.89%, respectively. The scatter plot of predicted removal efficiency by the M5 model versus measured data is illustrated in Figure 6.

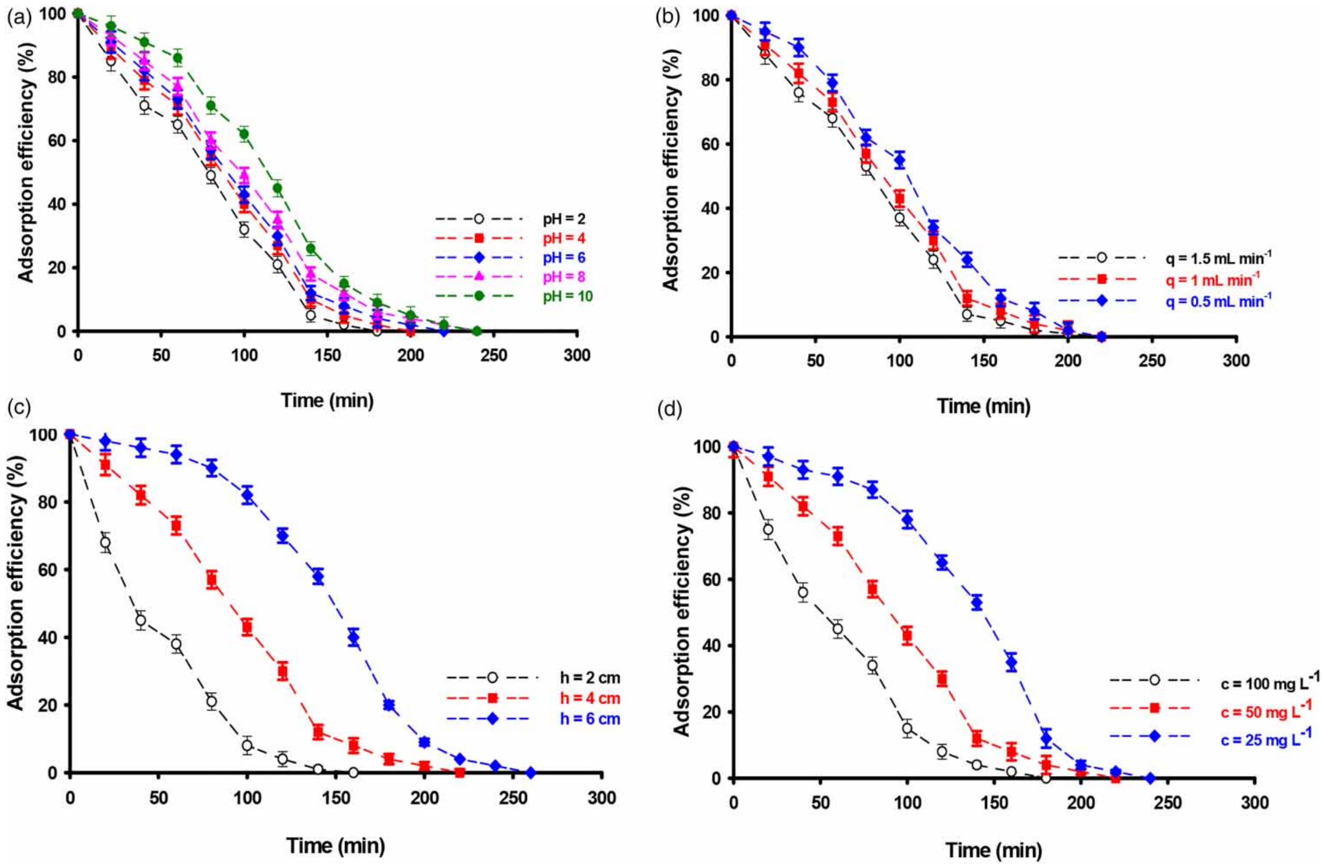


**Figure 4** | Removal efficiency of azithromycin in a fixed-bed column system as a function of pH (a), flow rates (b), bed depths (c), and initial concentrations (d).

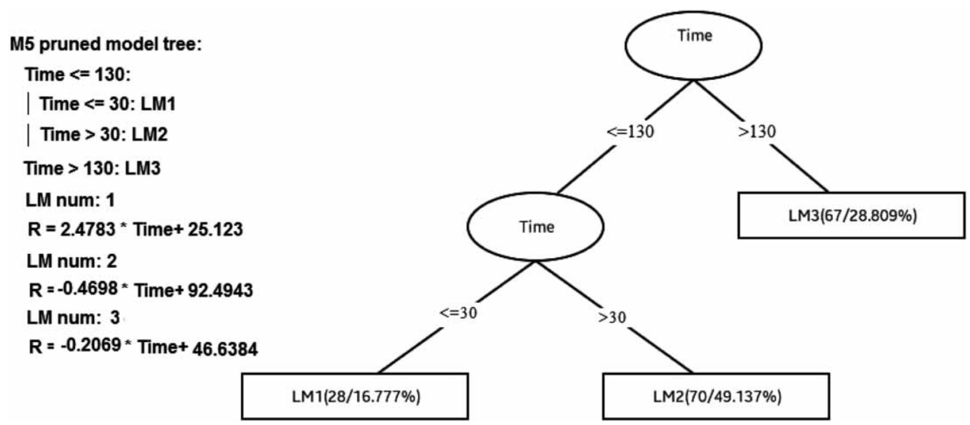


**Figure 5** | Linear models created by the M5 model tree.

Moreover, the estimation intervals at the 95% level, based on the distribution of points around the fitted line, demonstrate a good validity to predict the removal efficiency of azithromycin by MWCNTs. Results obtained from this study are in good agreement with the previous research, which showed the capabilities of the M5 model as an effective tool in modeling and approximating complex nonlinear systems in various fields such as reference evapotranspiration (Rahimikhoob 2014), sediment yield (Goyal 2014), and groundwater level (Nalarajan & Mohandas 2015). So, the outputs from the M5 model can compete with the other models such as the hybrid model (Amiri *et al.* 2019), the numerical approach (Amiri *et al.*

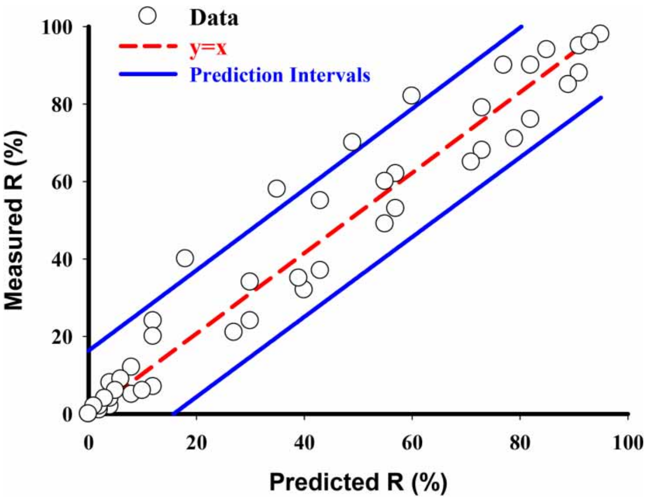


**Figure 6** | Scatter plot between measured predicted removal efficiency of azithromycin.

2018b), analytical approach (Amiri & Noshadi 2020), and artificial intelligence (Amiri *et al.* 2017b). However, in the application of the M5 model for adsorption modeling, this model cannot be used for multiple contaminations (i.e., competitive adsorption).

To check the obtained results from the M5 model, the experimental data were fitted to the Yoon–Nelson model, which is only a function of time, as follow (Deokar *et al.* 2016):

$$Ln\left(\frac{C_t}{C_0 - C_t}\right) = K_{YN}t - t_{0.5}K_{YN} \tag{6}$$

where $K_{YN}$ is the Yoon–Nelson kinetic model constant (min$^{-1}$) and $t_{0.5}$ is the time required for 50% azithromycin BT (min).

The predicted parameters of the Yoon–Nelson model ($K_{YN}$ and $t_{0.5}$) in the adsorption of azithromycin by MWCNTs as well as the $R^2$ at eleven series of column experiments are given in Table 1. The values of $K_{YN}$ were predicted between 0.032 and 0.043 min$^{-1}$ for various operating conditions, which were close to the average value of the $K_{YN}$ (0.035 min$^{-1}$). According to $R^2$ values ($R^2 > 0.962$), there is a satisfactory agreement between the predicted and measured $t_{0.5}$ values. Deokar *et al.* (2016) found that the predicted $t_{0.5}$ by the Yoon–Nelson model may be greater than measured values. The constant of $t_{0.5}$ is decreased with an increase in initial azithromycin concentrations and influent flow rates due to the driving force for mass

**Table 1** | Predicted kinetic parameters of Yoon-–Nelson model

| Expt. No. | $K_{YN}$ (min$^{-1}$) | $t_{0.5\ exp}$ (min) | $t_{0.5\ pre}$ (min) | $R^2$ |
|---|---|---|---|---|
| $E_1$ | 0.035 | 104 | 101.44 | 0.989 |
| $E_2$ | 0.034 | 94.09 | 88.15 | 0.996 |
| $E_3$ | 0.037 | 87.1 | 78.39 | 0.989 |
| $E_4$ | 0.043 | 49.49 | 41.64 | 0.977 |
| $E_5$ | 0.035 | 139.27 | 138.31 | 0.989 |
| $E_6$ | 0.039 | 78.72 | 71.54 | 0.962 |
| $E_7$ | 0.037 | 88.92 | 82.03 | 0.987 |
| $E_8$ | 0.032 | 102.74 | 97.07 | 0.997 |
| $E_9$ | 0.034 | 114.04 | 111.04 | 0.997 |
| $E_{10}$ | 0.035 | 60.03 | 52.21 | 0.993 |
| $E_{11}$ | 0.036 | 131.42 | 126.62 | 0.966 |

transfer, whereas $t_{0.5}$ is increased with an increase in pH and bed depth. Moreover, the unsymmetrical breakthrough curves were formed due to the intraparticle diffusion after 50% saturation of the column (Deokar *et al.* 2016). As seen in Supplementary Material, Figure S3, there is a good agreement between the predicted breakthrough curves using the Yoon–Nelson model and measured values under various operating factors. The results obtained from the Yoon–Nelson model confirmed the results from the M5 model, which revealed that the removal efficiency of azithromycin by MWCNTs in a continuous adsorption system is more sensitive to the contact time. The M5 model tree is more suitable than other models because this model generates simple and practical linear relations that can be easily applied by another user. Also, this model needs less computational time and is more convenient to use. Similar results were also seen by Rahimikhoob (2014), Goyal (2014), and Nalarajan & Mohandas (2015). The overall results are of significant practical use because the contact time can be used when other operational parameters are not available.

### Kinetic and equilibrium results

The kinetic and equilibrium models' parameters for azithromycin adsorption by MWCNTs are presented in Supplementary Material, Table S4. Results reveal that the Langmuir isotherm model fitted the equilibrium data better as the value of $R^2$ is 0.993 compared to the Freundlich isotherm model with a value of $R^2$ as 0.985, implying the homogeneous surface of the adsorbent. The maximum adsorption capacity calculated from the Langmuir isotherm model was 85.57 mg $g^{-1}$. The kinetic results indicated that the azithromycin adsorption mechanism follows the pseudo-second-order model ($R^2 = 0.998$), suggesting the chemical interactions between MWCNTs and azithromycin. So, chemical electrostatic attraction appears between the cationic species of azithromycin molecules and the negative surface of MWCNTs. The calculated uptake capacity obtained from the pseudo-second-order model (90.9 mg $g^{-1}$) is close to the maximum adsorption capacity calculated from the Langmuir isotherm model (85.57 mg $g^{-1}$).

## CONCLUSION

In this research, an alternative approach using the M5 model tree in predicting the efficiency of azithromycin antibiotics removal from continuous adsorption system by MWCNTs was examined. The removal percentage of azithromycin increased with increasing the bed depths and pH, whereas decreased by increasing the flow rate and initial azithromycin concentration. This study suggests that contact time is the most important parameter influencing the prediction of removal efficiency of azithromycin by MWCNTs using the M5 model tree as confirmed by the Yoon–Nelson model. The linear regression between the predicted adsorption efficiency by the M5 model tree and the observed values were proven to be satisfactory with an $R^2$ of 0.946 and RMSE of 9.89%. In view of the practical application, the M5 model tree can be used to predict nonlinear input–output relations of the adsorption process.

## CONFLICT OF INTEREST

The authors declare that they have no known competing financial interests or personal relationships that could have appeared to influence the work reported in this paper.

## DATA AVAILABILITY STATEMENT

All relevant data are included in the paper or its Supplementary Information.

## REFERENCES


Al-Riyami, I. M., Ahmed, M., Al-Busaidi, A. & Choudri, B. S. 2018 Antibiotics in wastewaters: a review with focus on Oman. *Applied Water Science* **8**, 199.

Alvarez-Elcoro, S. & Enzler, M. J. 1999 The macrolides: erythromycin, clarithromycin and azithromycin. *Mayo Clinic Proceedings* **74**, 613–634.

Amiri, M. J. & Noshadi, M. 2020 Evaluation of analytical and numerical solutions of mass transfer model for breakthrough curves simulation: $Co^{2+}$ adsorption by hydrogen peroxide-bio-originated composite. *Bioprocess and Biosystems Engineering* **43**, 1899–1910.

Amiri, M. J., Abedi-koupai, J. & Eslamian, S. 2017a Adsorption of Hg(II) and Pb(II) ions by nanoscale zero-valent iron supported on ostrich bone ash in a fixed-bed column system. *Water Science and Technology* **76**, 671–682.

Amiri, M. J., Abedi-Koupai, J., Jalali, S. M. J. & Mousavi, S. F. 2017b Modeling of fixed-bed column system of Hg (II) ions on ostrich bone ash/nZVI composite by artificial neural network. *Journal of Environmental Engineering-ASCE* **143**, 04017061.

Amiri, M. J., Bahrami, M., Beigzadeh, B. & Gil, A. 2018a A response surface methodology for optimization of 2,4-dichlorophenoxyacetic acid removal from synthetic and drainage water: a comparative study. *Environmental Science and Pollution Research* **25**, 34277–34293.

Amiri, M. J., Roohi, R. & Gil, A. 2018b Numerical simulation of Cd(II) removal by ostrich bone ash supported nanoscale zero-valent iron in a fixed-bed column system: utilization of unsteady advection-dispersion-adsorption equation. *Journal of Water Process Engineering* **25**, 1–14.

Amiri, M. J., Khozaei, M. & Gil, A. 2019 Modification of the Thomas model for predicting unsymmetrical breakthrough curves using an adaptive neural-based fuzzy inference system. *Journal of Water and Health* **17**, 25–36.

Amiri, M. J., Roohi, R., Arshadi, M. & Abbaspourrad, A. 2020 2,4-D adsorption from agricultural subsurface drainage by canola stalk-derived activated carbon: insight into the adsorption kinetics models under batch and column conditions. *Environmental Science and Pollution Research* **27**, 16983–16997.

Babaei, A. A., Lima, E. C., Takdastan, A., Alavi, N., Goudarzi, G., Vosoughi, M., Hassani, G. & Shirmardi, M. 2016 Removal of tetracycline antibiotic from contaminated water media by multiwalled carbon nanotubes: operational variables, kinetics, and equilibrium studies. *Water Science and Technology* **75** (4), 296–301.

Bahrami, M., Amiri, M. J., Mahmoudi, M. R. & Koochaki, S. 2017 Modeling caffeine adsorption by multi-walled carbon nanotubes using multiple polynomial regression with interaction effects. *Journal of Water and Health* **15** (4), 526–535.

Bahrami, M., Amiri, M. J. & Beigzadeh, B. 2018 Adsorption of 2,4-dichlorophenoxyacetic acid using rice husk biochar, granular activated carbon, and multi-walled carbon nanotubes in a fixed bed column system. *Water Science and Technology* **78**, 1812–1821.

Bassyouni, M., Mansi, A. E., Elgabry, A., Ibrahim, B. A., Kassem, O. A. & Alhebeshy, R. 2020 Utilization of carbon nanotubes in removal of heavy metals from wastewater: a review of the CNTs' potential and current challenges. *Applied Physics A* **126**, 38.

Cuerda-Correa, E. M., Alexandre-Franco, M. F. & Fernández-González, C. 2020 Advanced oxidation processes for the removal of antibiotics from water: an overview. *Water* **12**, 102.

Davoodi, S., Dahrazma, B., Goudarzi, N. & Gorji, H. G. 2019 Adsorptive removal of azithromycin from aqueous solutions using raw and saponin-modified nano diatomite. *Water Science and Technology* **80** (5), 939–949.

Deokar, S. K., Mandavgane, S. A. & Kulkarni, B. D. 2016 Adsorptive removal of 2,4-dichlorophenoxyacetic acid from aqueous solution using bagasse fly ash as adsorbent in batch and packed-bed techniques. *Clean Technologies and Environmental Policy* **18**, 1971–1983.

Dutta, A. K., Ghorai, U. K., Chattopadhyay, K. K. & Banerjee, D. 2018 Removal of textile dyes by carbon nanotubes: a comparison between adsorption and UV assisted photocatalysis. *Physica E: Low-Dimensional Systems and Nanostructures* **99**, 6–15.

Erto, A., Chianese, S., Lancia, A. & Musmarra, D. 2017 On the mechanism of benzene and toluene adsorption in single-compound and binary systems: energetic interactions and competitive effects. *Desalination and Water Treatment* **86**, 259–265.

Fonseca, E., Hernández, F., Ibáñez, M., Rico, A., Pitarch, E. & Bijlsma, L. 2020 Occurrence and ecological risks of pharmaceuticals in a Mediterranean river in Eastern Spain. *Environment International* **144**, 106004.

Gallo-Cordova, A., Castro, J. J., Winkler, E. L., Lima Jr, E., Zysler, R. D., del Puerto Morales, M., Ovejero, J. G. & Streitwieser, D. A. 2021 Improving degradation of real wastewaters with self-heating magnetic nanocatalysts. *Journal of Cleaner Production* **308**, 127385.

Gholamian, S., Hamzehloo, M., Farrokhnia, A. & Mahdavifar, Z. 2021 Response surface methodology optimizing the adsorptive removal of azithromycin using mesoporous silica SBA-15: mechanism, thermodynamic, equilibrium, and kinetics modeling studies. *Journal of Environmental Science and Health, Part A* **56** (10), 1145–1164.

Goyal, M. K. 2014 Modeling of sediment yield prediction using M5 model tree algorithm and wavelet regression. *Water Resource Management* **28**, 1991–2003.

Hu, A., Ren, G., Che, J., Guo, Y., Ye, J. & Zhou, S. 2020 Phosphate recovery with granular acid-activated neutralized red mud: fixed-bed column performance and breakthrough curve modelling. *Journal of Environmental Sciences* **90**, 78–86.

Kamani, H., Bazrafshan, E., Ashrafi, S. D. & Sancholi, F. 2017 Efficiency of Sono-nano-catalytic process of $TiO_2$ nano-particle in removal of erythromycin and metronidazole from aqueous solution. *Journal of Mazandaran University of Medical Sciences* **27**, 140–154.

Kim, H., Hwang, Y. S. & Sharma, V. K. 2014 Adsorption of antibiotics and iopromide onto single-walled and multi-walled carbon nanotubes. *Chemical Engineering Journal* **255**, 23–27.

Liu, Z., Hosseinzadeh, S., Wardenier, N., Verheust, Y., Chys, M. & Van Hulle, S. 2019 Combining ozone with UV and $H_2O_2$ for the degradation of micropollutants from different origins: lab-scale analysis and optimization. *Environmental Technology* **40** (28), 3773–3782.

Mohammadi, L., Rahdar, A., Khaksefidi, R., Ghamkhari, A., Fytianos, G. & Kyzas, G. Z. 2020 Polystyrene magnetic nanocomposites as antibiotic adsorbents. *Polymers* **12**, 1313.

Nalarajan, N. A. & Mohandas, C. 2015 Groundwater level prediction using M5 model trees. *Journal of The Institution of Engineers (India): Series A* **96** (1), 57–62.

Nghiem, L. D., Schäfer, A. I. & Elimelech, M. 2005 Pharmaceutical retention mechanisms by nanofiltration membranes. *Environmental Science and Technology* **39** (19), 7698–7705.

Pereira, A., Silva, L., Laranjeiro, C., Lino, C. & Pena, A. 2020 Selected pharmaceuticals in different aquatic compartments: part I – source fate and occurrence. *Molecules* **25**, 1026.

Qu, X., Alvarez, P. J. J. & Li, Q. 2013 Applications of nanotechnology in water and wastewater treatment. *Water Research* **47**, 3931–3946.

Quinlan, J. R. 1992 Learning with continuous classes. In *Proceedings of the Fifth Australian Joint Conference on Artificial Intelligence*, 16–18 November, Hobart, Australia. World Scientific, Singapore, pp. 343–348.

Rahimikhoob, A. 2014 Comparison between M5 model tree and neural networks for estimating reference evapotranspiration in an arid environment. *Water Resource Management* **28**, 657–669.

Rekhate, C. V. & Srivastava, J. K. 2020 Recent advances in ozone-based advanced oxidation processes for treatment of wastewater - a review. *Chemical Engineering Journal Advances* **3**, 100031.

Sadeghi, M., Sadeghi, R., Ghasemi, B., Mardani, G. & Ahmadi, A. 2018 Removal of azithromycin from aqueous solution using UV-light alone and UV plus persulfate (UV/$Na_2S_2O_8$) processes. *Iranian Journal of Pharmaceutical Research* **17** (2), 54–64.

Salvestrini, S., Fenti, A., Chianese, S., Iovino, P. & Musmarra, D. 2020 Diclofenac sorption from synthetic water: kinetic and thermodynamic analysis. *Journal of Environmental Chemical Engineering* **8**, 104105.

Takdastan, A., Mahvi, A. H., Lima, E. C., Shirmardi, M., Babaei, A. A., Goudarzi, G., Neisi, A., Heidari Farsani, M. & Vosoughi, M. 2016 Preparation, characterization, and application of activated carbon from low-cost material for the adsorption of tetracycline antibiotic from aqueous solutions. *Water Science and Technology* **74** (10), 2349–2363.

Uddin, S. 2021 Removal of pesticides using carbon-based nanocomposite materials. In: *Environmental Remediation Through Carbon Based Nano Composites. Green Energy and Technology* (Jawaid, M., Ahmad, A., Ismail, N. & Rafatullah, M., eds). Springer, Singapore. https://doi.org/10.1007/978-981-15-6699-8_17.

Wang, Y., Ma, J., Zhu, J., Ye, N., Zhang, X. & Huang, H. 2016 Multi-walled carbon nanotubes with selected properties for dynamic filtration of pharmaceuticals and personal care products. *Water Research* **92**, 104–112.

Witten, I. H. & Frank, E. 2005 *Data Mining: Practical Machine Learning Tools and Technique*. Morgan Kaufmann Publishers, San Francisco, p. 560.

Zhang, L., Song, X., Liu, X., Yang, L., Pan, F. & Lv, J. 2011 Studies on the removal of tetracycline by multi-walled carbon nanotubes. *Chemical Engineering Journal* **178**, 26–33.

First received 24 November 2021; accepted in revised form 7 March 2022. Available online 21 March 2022